Article

Not peer-reviewed version

Selective Paracrine Modulation of Stromal Cells: Wharton's Jelly MSC Secretome Enhances Adipose-Derived MSC Functionality While Maintaining Dermal Fibroblast Quiescence

Tanya Stoyanova , Lora Topalova , Stanimir Kyurkchiev , Regina Komsa-Penkova , Svetla Todinova , George Altankov *

Posted Date: 16 September 2025

doi: 10.20944/preprints202509.1359.v1

Keywords: Wharton's jelly MSCs; secretome; paracrine crosstalk; human adipose MSCs; primary fibroblasts; collagen interaction secretion; wound healing

 doi:10.20944/preprints202509.1359.v1

Article

Selective Paracrine Modulation of Stromal Cells: Wharton's Jelly MSC Secretome Enhances Adipose-Derived MSC Functionality While Maintaining Dermal Fibroblast Quiescence

Tanya Stoyanova [1,2], Lora Topalova [1,2], Stanimir Kyurkchiev [3], Regina Komsa-Penkova [2,4], Svetla Todinova [1] and George Altankov [2,5,6,*]

[1] Institute of Biophysics and Biomedical Engineering, Bulgarian Academy of Sciences, 1113 Sofia, Bulgaria
[2] Center of Competence in Personalized Medicine, 3D and Telemedicine, Robotic Assisted and Minimally Invasive Surgery at Medical University Pleven, 5800 Pleven, Bulgaria
[3] Tissue Bank BulGen, 1330 Sofia, Bulgaria
[4] Department of Biochemistry, Medical University-Pleven, 5800 Pleven, Bulgaria
[5] Associate Project BG-RRP-2.004-0003 at Medical University Pleven, 5800 Pleven, Bulgaria
[6] Research Institute at Medical University Pleven, 5800 Pleven, Bulgaria
* Correspondence: altankov@abv.bg

Abstract

Wharton's Jelly-derived mesenchymal stem cells (WJ-MSCs) secrete a rich array of paracrine factors including growth factors, cytokines, and extracellular vesicles that hold promises for regenerative medicine. This study evaluated the effects of WJ-MSC-derived secretome on adipose-derived mesenchymal stem cells (AD-MSCs) and human dermal fibroblasts (HDFs), focusing on their adhesion, spreading, proliferation, endogenous collagen secretion, and migration. Morphometric analysis revealed that the secretome enhanced cell adhesion and spreading on rat tail collagen (RTC) substrates after 24 hours. AD-MSCs showed a ~30% increase in cell spreading area (from 4007 μm² to 5081 μm² $p < 0.05$), though without notable shape changes. In contrast, fetal bovine serum (FBS) promoted cell elongation with reduced aspect ratio. Proliferation assays demonstrated a selective stimulatory effect of the secretome on AD-MSCs, with a significant increase at day 3, while HDFs' proliferation remained unchanged. Cell cycle profiling showed transient S-phase accumulation in AD-MSCs (24-48h), followed by G0/G1 arrest (72h), while HDFs remained in G0/G1. Immunofluorescence analysis confirmed enhanced extracellular deposition of endogenously synthesized collagen in AD-MSCs, while no comparable response was observed in HDFs. Scratch assays showed increased migration in both cell types upon secretome exposure, compared to collagen-only controls, suggesting a paracrine-mediated pro-migratory effect. These results demonstrate that WJ-MSC secretome boosts regenerative capacity in AD-MSCs while keeping fibroblasts quiescent, highlighting its strong potential for cell-free therapies in tissue engineering, wound repair, and regenerative medicine.

Keywords: Wharton's jelly MSCs; secretome; paracrine crosstalk; human adipose MSCs; primary fibroblasts; collagen interaction secretion; wound healing

1. Introduction

Mesenchymal stem cells (MSCs) are multipotent stromal cells capable of self-renewal and differentiation into various mesodermal lineages, including osteoblasts, chondrocytes, and adipocytes. First isolated from bone marrow, MSCs have since been identified in numerous tissues, such as adipose tissue, placenta, and umbilical cord, among others [1]. In the past decade, MSCs have

 doi:10.20944/preprints202509.1359.v1

emerged as a promising therapeutic modality in regenerative medicine due to their immunomodulatory properties, trophic support, and ability to home in on sites of tissue injury. Although initially believed to contribute to tissue repair through direct differentiation and engraftment, accumulating evidence suggests that their primary mechanism of action is mediated via paracrine signaling [2–4]. Following systemic or local administration, MSCs exhibit a transient lifespan often limited to 48–72 hours yet exert significant biological effects through the secretion of bioactive molecules, including cytokines, chemokines, growth factors, and extracellular vesicles such as exosomes [5]. These secreted factors, often termed secretome, play a pivotal role in modulating the local microenvironment, promoting angiogenesis, attenuating inflammation, and stimulating the activation and proliferation of endogenous stem and progenitor cells [3,6]. Consequently, the regenerative outcomes observed in MSC-based therapies are increasingly attributed to the indirect activation of host repair mechanisms, rather than the direct cellular replacement by the transplanted MSCs themselves [4]. This paradigm shift underscores the importance of understanding the molecular composition and functional relevance of the MSC secretome in order to optimize therapeutic efficacy and design next-generation cell-free regenerative strategies.

Among the various MSC sources, Wharton's Jelly—the gelatinous connective tissue within the umbilical cord—has emerged as a particularly promising reservoir of MSC as they are easily accessible, ethically non-controversial, and exhibit high proliferative capacity and low immunogenicity. Accumulating evidence suggests a unique therapeutic potential of Wharton's Jelly-derived mesenchymal stem cells (WJ-MSCs) [7–9], which have recently led to growing commercial interest. Several companies now offer cryopreserved WJ-MSCs collected at birth, with the intention of future therapeutic use for the donor child [10–12]. Emerging research, however, increasingly indicates that the actual therapeutic efficacy of Wharton's Jelly MSC, is similarly attributed to their paracrine activity—namely, the bioactive molecules they secrete collectively rather than through direct cellular engraftment or replacement [7,13,14]. Indeed, Wharton's Jelly MSC secretome encompasses a complex mixture of soluble proteins, cytokines, chemokines, growth factors, and extracellular vesicles (EVs), including exosomes and microvesicles (Trigo et al., 2025). These bioactive components modulate inflammation, promote angiogenesis, and support tissue repair and regeneration. Though the composition and potency of the secretome vary depending on the MSC source, WJ-MSCs demonstrate a particularly rich and functionally diverse profile [17].

As interest in cell-free regenerative therapies continues to accelerate, the secretome derived from WJ-MSCs has gained recognition as a promising, scalable, and low-risk alternative to direct cell transplantation [7]. While its therapeutic potential is increasingly acknowledged, the ability of WJ-MSC secretome to influence the behavior of other mesenchymal stem cell populations such as adipose-derived MSCs (AD-MSCs) remain insufficiently explored. Likewise, its effects on other adult cell types, particularly fibroblasts, which are key players in tissue repair and remodeling, are still poorly understood [18]. Indeed, recent advances have reshaped our understanding of MSCs interactions with fibroblasts, particularly in the context of fibrosis. A pivotal study by Xu and colleagues (2023) [19] demonstrated that MSCs can reversibly de-differentiate myofibroblasts back into fibroblast-like cells by selectively inhibiting the TGF-β–SMAD2/3 signaling pathway, a central axis in fibrotic progression. This finding challenges the long-held notion that myofibroblasts are terminally differentiated and opens new therapeutic avenues for treating fibrotic diseases such as idiopathic pulmonary fibrosis and bronchiolitis obliterans. Importantly, Xu et al. (2023) [19] revealed that these de-differentiated fibroblast-like cells retain sensitivity to TGF-β1 and can re-enter the myofibroblast state if the pro-fibrotic microenvironment persists. This underscores the need for sustained modulation of the niche and highlights the dynamic plasticity of fibroblast phenotypes under MSC influence. Similar observations were made by Dyachkova and colleagues (2023) [20], who showed that chronic inflammation mediated by M2 macrophages can induce reversible senescence in MSCs, thereby affecting their anti-fibrotic properties. These insights deepen our mechanistic understanding of MSC-fibroblast crosstalk and provide a rationale for the variable clinical outcomes observed in MSC-based therapies for fibrotic conditions. Earlier work by Desai, Hsia, and

 doi:10.20944/preprints202509.1359.v1

Schwarzbauer (2014) [21] also supports the concept of reversible modulation of myofibroblast differentiation, demonstrating that adipose-derived MSCs can influence fibroblast phenotype in a context-dependent manner. Together, these studies highlight the therapeutic potential of MSCs not only as regenerative agents but also as dynamic modulators of fibrotic remodeling.

A key question arises in the context of cell-free regenerative therapies: are there significant differences between the secretomes of WJ-MSCs and AD-MSCs? Comparative studies have indeed revealed distinct variations in their secretory profiles. Proteomic analyses show that WJ-MSCs secrete a broader and more potent array of bioactive molecules, including high levels of immunomodulatory cytokines such as IL-10, TGF-β, and HGF, as well as pro-regenerative factors like VEGF, IGF-1, and FGF-2. In contrast, AD-MSCs tend to produce a more tissue-specific secretome, with relatively higher concentrations of IL-6, MCP-1, and MMPs, which support localized repair but offer limited systemic paracrine signaling [7,13,17,22]. Mechanistically, the regenerative potential of WJ-MSCs shall be largely attributed to their paracrine activity, involving the secretion of the above key bioactive molecules. These factors play crucial roles in angiogenesis, fibroblast recruitment, ECM remodeling, and immunomodulation [7,22]. VEGF promotes endothelial cell proliferation and neovascularization, PDGF supports mesenchymal cell migration and matrix deposition, while TGF-β is central to wound healing and fibrosis regulation. The coordinated release of these molecules by WJ-MSCs underscores their superior paracrine signaling capacity and positions them as a promising cell-free therapeutic source.

These molecular distinctions are particularly relevant for regenerative medicine, as the composition of the secretome can critically influence therapeutic efficacy. WJ-MSCs, with their enriched profile of anti-inflammatory and angiogenic factors, may be better suited for treating systemic inflammatory conditions and promoting tissue regeneration across diverse organ systems. Meanwhile, AD-MSCs may offer advantages in targeted therapies where localized tissue remodeling is desired.

Equally underexplored is the role of the surrounding extracellular matrix (ECM), especially collagen, the primary structural protein within it. Collagen contributes to tissue regeneration not only by offering mechanical support but also by delivering essential biochemical signals that facilitate effective cellular interactions. In stem cell biology, collagen enhances adhesion, survival, and proliferation, while also influencing differentiation pathways through integrin-mediated and other signaling mechanisms [23–25]. All types of MSCs are particularly responsive to collagen-rich microenvironments, which promote better engraftment and drive lineage-specific differentiation—most notably toward osteogenic, chondrogenic, and adipogenic outcomes [26]. Furthermore, collagen serves as a bioactive scaffold that closely replicates the native ECM, facilitating key cellular processes such as stem cell migration, spatial organization, and tissue remodeling, essential for successful regenerative therapies [27–29]. These regenerative dynamics can be effectively assessed in vitro using the artificial wound healing (scratch) assay—a widely accepted technique for quantifying cell migration and matrix remodeling [30]. In this study, we applied the scratch assay to investigate the influence of WJ-MSC secretome on the migratory behavior of both AD-MSCs and fibroblasts cultured on collagen-coated substrates. This builds upon our previous methodological framework [25,31], which demonstrated MSC-mediated remodeling of adsorbed collagen under oxidative stress or high glucose conditions using both morphological and morphometric analyses. Together, these approaches highlight the responsiveness of MSCs to microenvironmental cues and underscore their relevance in modeling pathological tissue repair. They also show that collagen is not merely a passive scaffold; it undergoes active remodeling through interactions between stem cells and fibroblasts, contributing to its dynamic turnover within tissues. This remodeling is particularly pronounced during wound healing and regeneration, where collagen serves not only as a structural matrix but also as a signaling platform that orchestrates new tissue formation [32,33].

This study aimed to systematically evaluate the effects of the WJ-MSC secretome on key functional parameters of AD-MSCs and in a comparative plan on primary human fibroblasts. Emphasis was placed on cell adhesion to adsorbed rat tail collagen (RTC), distinctly assessed from

 doi:10.20944/preprints202509.1359.v1

the intracellular collagen by using species-specific antibodies visualized through immunofluorescence. Additional endpoints included quantitative analysis of cell morphology, proliferative activity, and cell cycle dynamics of both cell types, alongside assessment of their migratory behavior using an in vitro scratch wound assay.

2. Materials and Methods

2.1. Cells

Human adipose tissue derived mesenchymal stem cells (AD-MSCs) at passage 2 were obtained from the Tissue Bank BulGen (Sofia, Bulgaria) with informed consent from donors prior to liposuction. Cells were cultured in DMEM/F12 medium supplemented with 10% fetal bovine serum (FBS) (both from Sigma-Aldrich, USA) and 1% antibiotic–antimycotic solution (Sigma-Aldrich, USA) in humidified thermostat at 37 °C, 5% CO_2. Medium was replaced every 2 to 3 days until cells reached ~90% confluence and then passaged using 0.05% trypsin/0.6 mM EDTA (Sigma-Aldrich, USA). Cells used for experiments were between passages 5 and 7.

Primary human dermal fibroblasts (HDFs) were isolated from fresh skin biopsy also with informed donor consent following the procedure of Ningsih [34]. Briefly, the donor skin was sectioned into approximately 2x2 mm fragments, left to attach in a 12-well TC polystyrene plate (Corning, USA) on a marked by scratches area, done to enhance the cell attachment. The explants were cultured in DMEM/F12 medium supplemented with 10% FBS (Sigma-Aldrich, USA) and 1% antibiotic–antimycotic solution (Sigma-Aldrich, USA) in humidified thermostat at standard conditions (37 °C, 5% CO_2). Once fibroblasts began migrating out of the explant, the culture medium was replaced every 3–5 days. Primary cultures were maintained for approximately 10 days, until reaching ~70–80% confluence. Cells were then harvested with trypsin–EDTA solution (Sigma-Aldrich, USA), and its activity was neutralized by adding an equal volume of FBS, then the cell suspension was centrifuged at 300 × g for 5 min. The pellet was resuspended in fresh medium and seeded in a T25 TC polystyrene flask (Corning, USA) and left for subsequent cultivation in standard conditions.

2.2. Preparation of Collagen-Coated Surfaces

Collagen type I was produced from rat tail tendon by acetic acid extraction and salting out with NaCl, as described elsewhere [35]. The pellets were collected by centrifugation at 4000 rpm at 4 °C for 30 min and re-dissolved in 0.05 M acetic acid, then dialyzed to remove the excess NaCl. All procedures were performed at 4 °C. The collagen concentration in the solutions was measured by the modified Lowry assay [36] and from the optical absorbance at 220–230 nm.

Collagen-coated 24-well culture plates (Greiner Bio-One, Germany) or 22x22 mm glass coverslips (ISOLAB GmbH, Germany, placed in 6 well plates), were coated with 100 μg/mL rat tail collagen (isolated as above) dissolved in 0.05 M acetic acid via incubation at 37 °C for 1 h, before samples were rinsed three times with phosphate buffered saline (PBS).

2.3. Secretome Treatment

AD-MSCs and HDFs were seeded at 1.2 × 10^4 cells/well in 600 μL of serum-free medium on collagen-coated 24-well plates or alternatively on coverslips in 6 well plates. After 2 h of incubation (37 ^{O}C, 5% CO2), WJ-MSCs' secretome was added in final protein concentration of 0.03 mg/ml. Control groups received only serum-free medium as a negative control or medium supplemented with 10% FBS as a positive control.

 doi:10.20944/preprints202509.1359.v1

2.4. Cell Proliferation Assay

Cell proliferation was assessed at 24, 48, and 72 h of culture. Cells were fixed with 4% paraformaldehyde and stained with Hoechst 33258 (1:2000, Sigma-Aldrich) to visualize cells Nuclei then viewed at fluorescence microscopy (Thunder Imager Live Cell, Leica) with a 10x objective and counted using the CellProfiler software [37]. The doubling time was calculated by using the following formula:

$$\text{Doubling Time} = [T \times (\ln 2)] / [\ln (N_e/N_b)],$$

where N_b is the initial cell density, N_e is the final cell density and T is the time passed between the two measurements.

2.5. Cell Cycle Analysis

Cell cycle distribution was determined in accordance with the protocol of Vassilis Roukos [38]. Briefly, the fluorescent images were taken on a fluorescent microscope with 10x objective. Then a pipeline provided by the team of Roukos was applied to the image set which allowed the quantification of the DNA in each nucleus. The Cell cycle analysis was performed using Floreada.io (https://floreada.io/) where nuclei were classified into 3 groups according to the cell cycle phase (G1/G0, S, G2/M) and plotted in 3 colored graphs.

2.6. Morphological Analysis and Endogenous Collagen Production

After 24h of incubation in defined conditions HDFs and MSCs were fixed in 4% paraformaldehyde and permeabilized with 0.5% Triton X-100 for 5 min before washed and treated with blocking solution (PBS with 10% FBS (Sigma-Aldrich, USA), 15 min), then incubated (37°C) with rabbit anti-human collagen 1 (AB745, Sigma-Aldrich, USA) followed by Alexa Fluor® 555-conjugated donkey anti-rabbit IgG (406412, BioLegend) as secondary antibody. All antibodies were applied in 1:100 dilution in PBS containing 10% FBS (Sigma-Aldrich, USA). The actin cytoskeleton was visualized using Alexa Fluor™ 488 phalloidin (Invitrogen), and the nuclei were counterstained with Hoechst 33258 (1:2000). Fluorescent images were acquired using a fluorescence microscope (Thunder Imager Live Cell, Leica) with 20x objective. In order to determine the overall cell shape the CellProfiler software [37] was used.

2.7. Artificial Wound Healing (Scratch) Assay

MSCs and HDFs were seeded in 12-well plates and incubated until rich around confluent cell density (90%) when a linear scratch was made across the cell monolayer using a sterile 200 µL pipette tip. The samples were studied either plain (medium only), or medium supplemented with 10% WJ-MSCs secretome (from 10X concentrate), or with 10% FBS as positive control. The cells were incubated using live cell chamber of the inverted microscope (Thunder Imager Live Cell, Leica) in time-laps mode (each 15 min) during 24 h. Images of the wound area were captured in a selected time points (0 and 24 h) with 10X objective under phase-contrast.

The wound area was quantified using ImageJ software with a plugin for the high throughput image analysis of in vitro scratch assays [39] and the percentage of wound closure was calculated as:

$$\%\ Closure = [(A_0 - A_t) / A_0] \times 100,$$

where A_0 is the wound area at 0 h and A_t is the area at time t.

2.8. Statistical Analysis

Statistical analysis was done using GraphPad Prism 8 (GraphPad Software, USA). After test for normality was performed, the data was analyzed with one-way analysis of variance (ANOVA),

 doi:10.20944/preprints202509.1359.v1

followed by a correction for multiple comparisons Tukey's Honest Significant Difference test. Results were displayed as column bar graphs, as scatter plots with each point representing an independent replicate, as line graphs, or as percentage stacked bar chart. Mean ± SEM (or SD) is indicated as described in the figure legends. The confidence limit reflecting the significant difference between experimental groups was considered 95%, when $p < 0.05$.

3. Results

3.1. Effect of the WJ-MSCs' Secretome on the Morphology of AD-MSCs and Fibroblasts

Aligned with the central aim of this study, we initially explored the impact of the Wharton's Jelly secretome (WJ-MSCs) on the adhesion and morphological characteristics of adipose-derived mesenchymal stem cells (AD-MSCs) and human dermal fibroblasts (HDFs), all originating from distinct mesenchymal tissues. Collagen was selected as the substrate protein due to its prominent role as a key ECM component, essential for tissue regeneration and the whole stem cell biology field [26].

As depicted in Figure 1/Panel A, exposure to WJ-MSC-derived secretome administered at a concentration equivalent to that present in the native WJ-MSC culture medium resulted in enhanced cell spreading of both AD-MSCs and HDFs after 24 hours of incubation (Figure 1A(b) and 1A(e), respectively), compared to cells cultured on collagen-only substrates (Figure 1A(a) and 1A(d)). Notable differences in cytoskeletal architecture were also observed. For AD-MSC samples, incubation with secretome led to the development of prominent actin stress fibers, indicating enhanced cytoskeletal organization. Conversely, samples treated with FBS showed less pronounced stress fibers formation, characterized by a primarily cortical arrangement, while cells grown on plain collagen revealed an intermediate cytoskeletal phenotype (Figure 1A(a-c)). Fibroblasts, in the same conditions, exhibited less developed actin networks compared to AD-MSCs, while treatment with FBS induced more polarized morphology in both cell types (Figure 1A(c) and 1A(f)), suggesting differential modulation of cytoskeletal dynamics depending on the bioactive environment. In this respect, it is important to note that these morphological characteristics were assessed after 24 hours of incubation—a time point where the organization of actin cytoskeleton differs significantly from the early stages of cell adhesion.

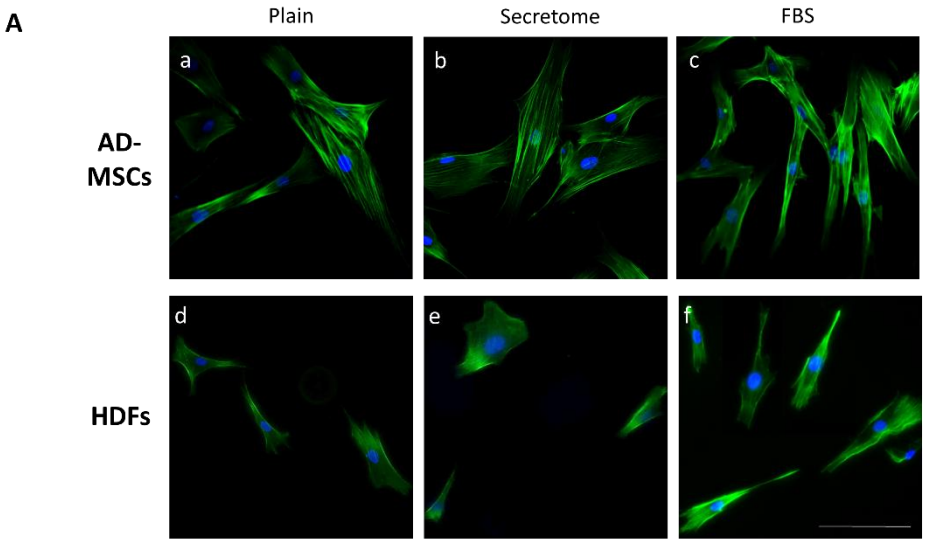

 doi:10.20944/preprints202509.1359.v1

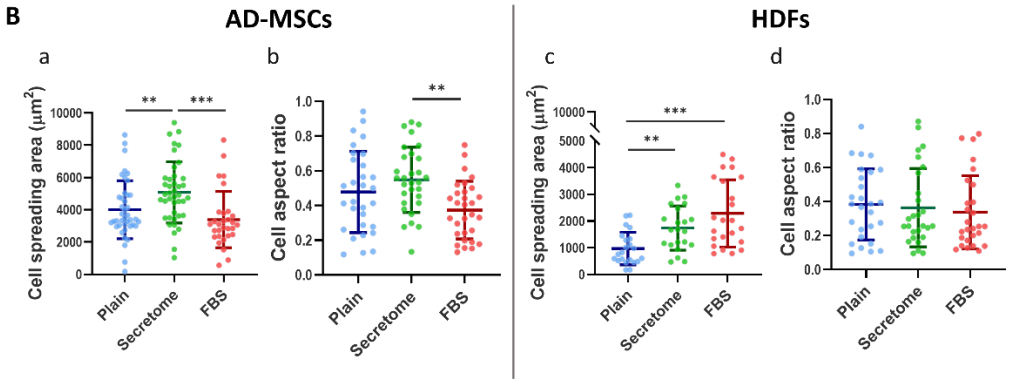

Figure 1. Wharton's Jelly-derived mesenchymal stem cells **(**WJ-MSCs) secretome affects the morphology of adipose tissue derived MSCs and HDFs adhering on collagen-coated substrates. Panel A: Representative images of adipose-derived mesenchymal stem cells (AD-MSCs) (a–c) and human dermal fibroblasts (HDFs) (d–f) cultured for 24 hours on collagen-coated surfaces under different conditions, namely: (a, d) Untreated control cells (Plain); (b, e) cells cultured in presence of WJ-MSC-derived secretome; and (c, f) cells cultured in the presence of 10% fetal bovine serum (FBS) (positive control). Cells were stained with phalloidin (green) to visualize F-actin and Hoechst (blue) for nuclear DNA. Panel B: Quantitative morphometric analysis of cell morphology including cell spreading area and aspect ratio of AD-MSC (a, b) and HDF (c, d). The data are presented as mean ± SEM. Asterix denotes statistical significance: $p < 0.05$ (*), $p < 0.01$ (**), $p < 0.001$ (***). Scale bar in A: 50 μm.

Quantitative morphometric analysis shown on Figure1/Panel B and Table 1) revealed statistically significant differences in cell spreading area (CSA) and cell aspect ratio (AR) for both AD-MSCs and HDFs (Figure 1/ Panel B). In the presence of WJ-MSC secretome, AD-MSCs exhibited a ~30% increase in CSA, expanding from 4007 μm² on unmodified collagen to 5081 μm² (Figure 1B(a)), indicative of enhanced cell-substrate interaction. This expansion was accompanied by an approximate 15% increase in AR, suggestive of slightly diminished cellular polarization. Conversely, under serum-enriched conditions (the positive control), AD-MSCs demonstrated a ~15% reduction in CSA, decreasing to 3389 μm² from the baseline of 4007 μm² (Figure 1B(a)), which was correlated with a concomitant decrease in AR values (Figure 1B(b); Table 1), implying increased cellular elongation and potential directional migration.

Table 1. Quantitative cell morphology averages of Cell Spreading Area in μm² (CSA) and Cell Aspect ratio (AR), varying from 1 (for circle) to 0 (for extended line) and characterizing cell polarization.

	Condition	Average Cell Spreading Area (CSA) μm²	Deviation from the Control of CSA (%)	Average Aspect Ratio (AR)	Deviation from the Control of AR (%)
AD- MSCs	Plain (Control)	4007	-	0.4781	-
	Secretome	5081	26.8	0.548	14.6
	FBS	3389	-15.4	0.3736	-21.9
HDFs	Plain (Control)	971.6	-	0.3825	-
	Secretome	1737	78.8	0.3634	-5.0
	FBS	2289	135.6	0.337	-11.9

Fibroblasts, typically over threefold smaller in size compared to AD-MSCs, also demonstrated enhanced spreading in the presence of WJ-MSC secretome, with CSA increasing by approximately 79%, from 971.6 μm² to 1737 μm² (Figure 1B(c)). Despite this improvement, their CSA remained intermediate and did not reach the values observed in fibroblasts cultured with FBS, where a CSA of

 doi:10.20944/preprints202509.1359.v1

2289 μm² was recorded (corresponding to a 135.6% increase). AR values for fibroblasts remained relatively stable at around 0.350 (Table 1), showing only modest decreases ranging from 5% to 11.9% compared to controls, indicating a slight increase in cellular polarization (Figure 1A (e and f)).

3.2. WJ-MSC Secretome Supports the Growth of MSCs, but not of Fibroblasts

Building upon our preliminary findings that WJ-MSC-derived secretome enhances the proliferation of AD-MSCs, we now provide a more comprehensive analysis of this effect, including a comparative evaluation of its influence on fibroblasts. This approach is motivated by the involvement of both cell types in tissue regeneration and the clear relevance of this experimental observation to regenerative medicine.

As shown in Figure 2A, the WJ-MSC-derived secretome promotes the proliferation of AD-MSCs cultured on collagen substrates under serum-free conditions, with a statistically significant effect observed by day 3.

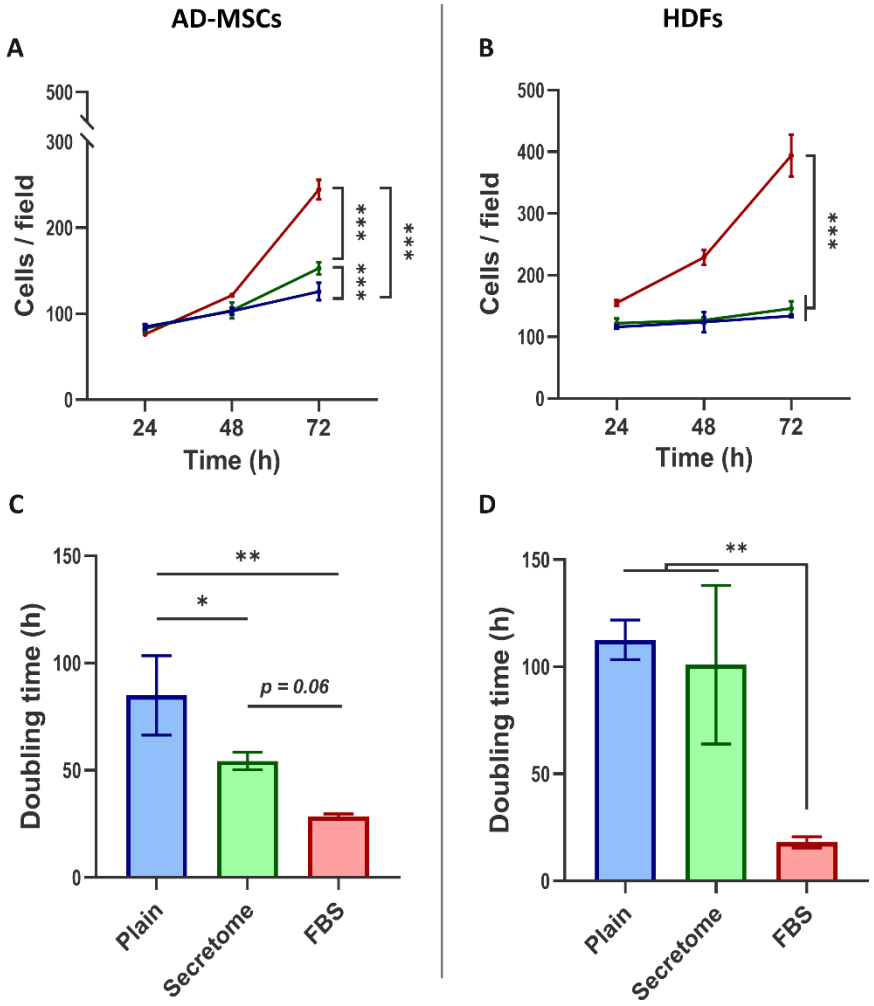

Figure 2. WJ-MSCs' secretome enhances cell proliferation and reduces doubling time in AD-MSCs, but has no effect on HDFs, when cultured on collagen-coated surfaces. Graphs A and C show proliferation dynamics of AD-MSCs presented as cells per field, while B and D—of HDFs. The cells were cultured for 72 hours on collagen-coated substrata in serum-free medium (blue), or such supplemented with either WJ-MSC-derived secretome (green), or with 10% FBS (red). (A) The cell number was quantified at 24, 48, and 72 hours (A and B) while Cell Doubling Time was calculated over the full 72-hour period (C, D). For graphs A and B, statistical analysis was performed at the final time point (72 h). All data are presented as mean ± SEM. Asterix denotes statistical significance: $p < 0.05$ (*), $p < 0.01$ (**), $p < 0.001$ (***).

 doi:10.20944/preprints202509.1359.v1

In contrast, HDFs cultured under identical conditions did not exhibit a notable increase in cell number (Figure 2B), except in the presence of FBS, where cell counts were significantly elevated on both day 2 and day 3, reaching approximately double the control levels by day 3 for both cell types.

The influence of secretome on the cell proliferation kinetics is more clearly illustrated by analyzing the cell doubling time (Figure 2C and 2D). For AD-MSCs, secretome treatment resulted in a substantial reduction in doubling time, approximately twofold compared to controls (Figure 2C), again indicating an accelerated proliferation. However, no significant change in cell doubling time was observed for HDFs under the same conditions (Figure 2D). In both cell types, FBS supplementation consistently yielded the shortest doubling times, confirming its potent mitogenic effect.

3.3. Impact of Paracrine Signaling from WJ-MSCs on Cell Cycle Progression in Stem Cells and Fibroblasts

To better clarify the effect of WJ-MSCs' secretome we further performed an Image based fluorocytometric analysis of the nuclear DNA content as viewed by Hoechst staining of the same AD-MSC and HDF cells cultured for 24, 48, and 72 hours. WJ-MSCs' secretome treatment leads to faster proliferation in stem cells compared to the control with plain media, observable on the 48h and more so on the 72h after the start of the incubation, whit a doubling time 1.6 times faster than that of the non-treated samples, but still about 1.9 times slower than the cells with incubated with FBS 10%. This tendency was not present when fibroblasts were treated with secretome, where no difference was found in the proliferation rate.

As shown in Figure 3, the WJ-MSC-derived secretome exerts distinct modulatory effects on cell cycle progression in MSCs, while having minimal impact on HDFs. MSCs exposed to secretome under serum-free conditions display a transient accumulation in the S phase at 24 and 48 hours, followed by a pronounced shift toward G0/G1 by 72 hours, indicative of entry into a quiescent state. In contrast, fibroblasts treated with secretome remain consistently arrested in the G0/G1 phase throughout the entire observation period, with no detectable transition into S or G2/M phases. These cell cycle profiles are consistent with the previously noted differences in cell proliferation and doubling time.

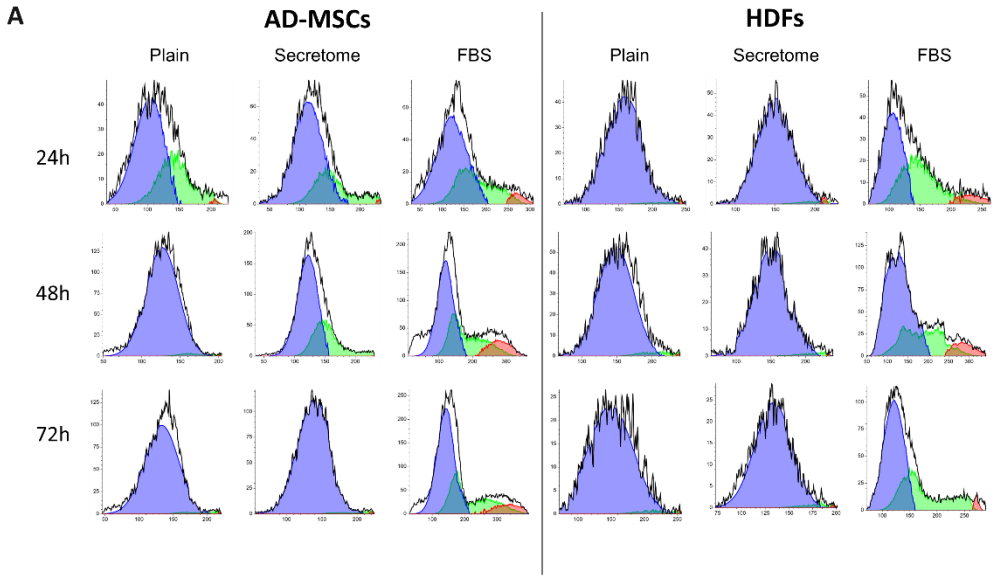

 doi:10.20944/preprints202509.1359.v1

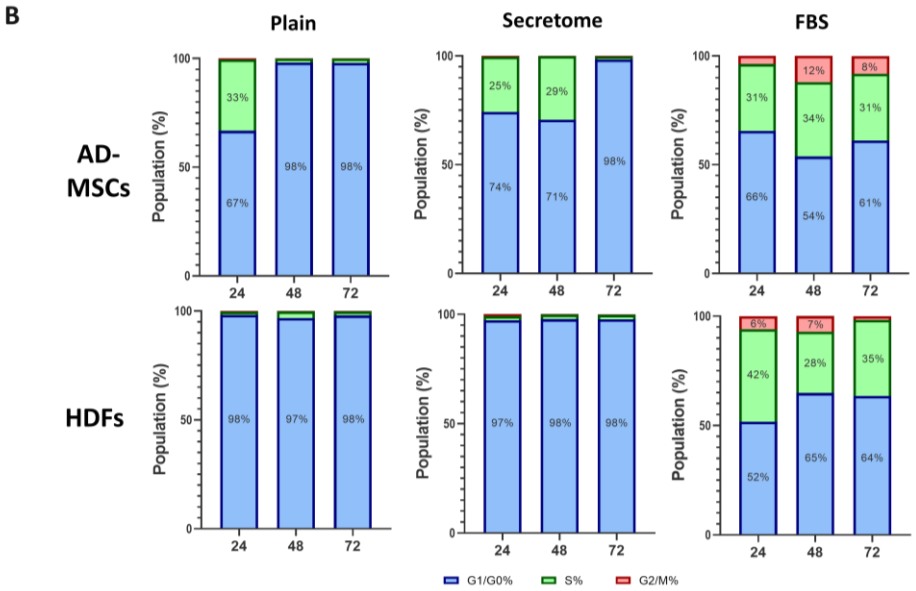

Figure 3. WJ-MSC secretome selectively modulates cell cycle progression in MSCs, but not in HDFs, cultured on collagen-coated substrates. Fluorocytometric analysis of nuclear DNA content was performed using Hoechst staining in AD-MSCs and HDFs cultured for 24, 48, and 72 hours under three conditions: plain medium (Control), medium supplemented with WJ-MSC-derived secretome (Secretome), and medium supplemented with 10% FBS. Panel A displays representative DNA histograms, where event count (y-axis) is plotted against total nuclear fluorescence intensity (x-axis), reflecting DNA content. Cell cycle phases are color-coded: G0/G1 (blue), S (green), and G2/M (red). AD-MSCs and HDFs were analyzed at each time point (24 h, 48 h, and 72 h), with conditions indicated as Control (plain medium), Secretome (WJ-MSC-derived secretome), and FBS (10% FBS supplementation). Panel B presents quantitative analysis of cell cycle phase distribution, expressed as a percentage of the total cell population for AD-MSCs (left) and HDFs (right). Color coding is consistent across the two panels.

3.4. Paracrine Signaling from WJ-MSCs Modulates Extracellular Collagen Deposition

A key hallmark of mesenchymal cell function is the production and organization of the ECM [40], with collagen playing a central role. In this context, we investigate the influence of the WJ-MSC secretome on the intracellular processing and substratum deposition of collagen by AD-MSCs and HDFs, again in comparative plan. Specifically, we examine the fate of the endogenous type I collagen produced by these cells using an anti-human collagen antibody, while they are cultured on a RTC, which is not detected by the antibody.

Figure 4 illustrates the intracellular organization and extracellular deposition of endogenous human type I collagen following 24-hour incubation of AD-MSCs (Panel A) and HDFs (Panel B) on RTC-coated substrata. The impact of WJ-MSC secretome (Images on Figure 4A (b, f) and 4B (b, f) is assessed relative to plain collagen-coated controls (Figure 4A (a, d) and 4B (a, d)) and FBS supplementation (Figure 4A (c, g) and 4B (c, g)), which serves as a positive control.

In both A and B panels, the bottom row displays the same cells as on the top row, but with outlined contours to delineate intracellular and extracellular compartments—an essential distinction for the subsequent microfluorimetric quantifications shown in diagrams (d and h) on both panels (A and B), respectively.

Analysis of Panel A revealed that the WJ-MSC secretome significantly enhanced extracellular deposition of collagen type I by AD-MSCs. This was evidenced by the clustered fluorescence signals (indicated by an arrow in image b on Panel A) and quantitatively supported by elevated fluorescence intensity (images d and h on Panel A). The deposited collagen appeared morphologically disorganized, forming dense clusters without clear spatial alignment (see 5x augmented inset on image b). These differences were statistically significant, as shown in graph (A (d)).

 doi:10.20944/preprints202509.1359.v1

In contrast to AD-MSCs, HDFs cultured under identical conditions (Panel B) demonstrated significantly lower levels of extracellular collagen type I deposition in response to the WJ-MSC secretome (images B (b) and (f)). This reduction was evident when compared to both the plain collagen control (images B (a) and (e)) and the FBS-supplemented samples (images B (c) and (g)), with statistical significance confirmed in graph B d.

Additionally, intracellular collagen fluorescence in both cell types (Panels A and B) exhibited a consistent perinuclear localization. The fluorescence intensity remained intermediate between the plain collagen and FBS-supplemented conditions, with no statistically significant differences observed (Panels A (h) and B (h)). This distribution pattern is morphologically indicative of Golgi-associated intracellular processing.

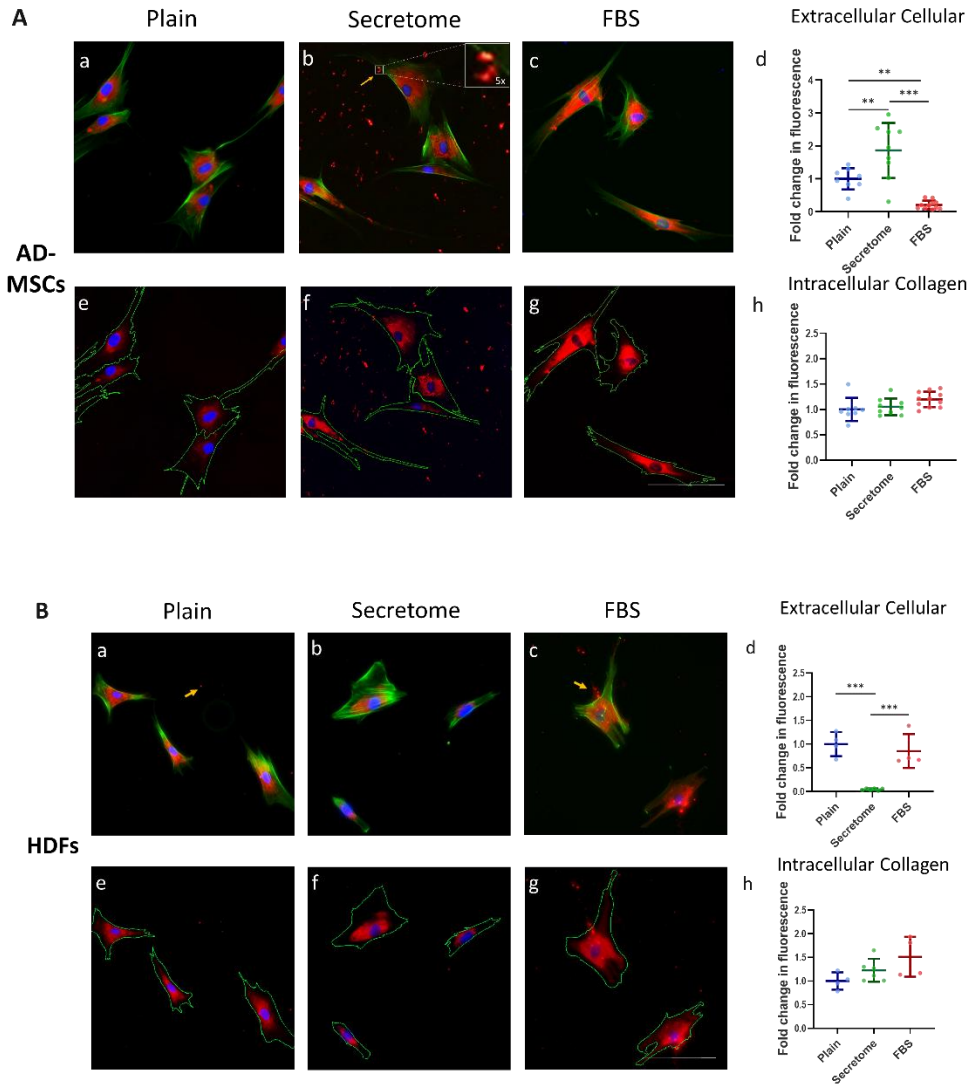

Figure 4. WJ-MSC secretome differentially regulates extracellular collagen deposition by MSCs and HDFs. Immunofluorescence imaging and quantitative analysis of collagen type I localization in AD-MSCs (Panel A) and HDFs (Panel B) cultured under three conditions: serum-free control (Plain; images (a, e)), WJ-MSC-derived secretome (Secretome; images (b, f)), and 10% FBS supplementation (FBS; images (c, g)). Panel A (a–c) shows representative triple-stained images for nuclei (Hoechst, blue), F-actin (phalloidin, green), and collagen I (Alexa Fluor 555, red). Corresponding images (e–g) display collagen and nuclei only, with cell borders overlaid (based on cytoskeletal contours) to enable segmentation and quantification of intra- and extracellular collagen. Yellow arrows indicate extracellular collagen deposits. Inset in Panel A(b) displays a 5× magnified view of secreted collagen, highlighting its clustered morphology. Quantitative analysis of extracellular collagen fluorescence, normalized to cell number, is shown in graphs A(d) for AD-MSCs and B(d) for HDFs. Intracellular collagen

 doi:10.20944/preprints202509.1359.v1

levels are presented in A(h) and B(h), expressed as fold change relative to control. Statistical significance is indicated as follows: $p < 0.05$ (*), $p < 0.01$ (**), $p < 0.001$ (***). Scale bar: 100 µm.

3.5. WJ-MSC Secretome Enhances Migration of both Stem Cells and Fibroblasts

Another essential hallmark of the regenerative potential of mesenchymal stem cells and fibroblasts is their capacity for directed migration toward sites of tissue injury—an ability that can be effectively simulated using the in vitro wound healing assay, commonly referred to as the scratch assay [41]. Figure 2 illustrates the impact of the WJ-MSC-derived secretome on the migratory behavior of AD-MSCs and HDFs, as evaluated through time-lapse microscopy of live cells (see Methods section and Supplementary Movies S1A–S1C). The figure presents only representative images captured at the initiation of the assay and following 24 hours of incubation.

As can be seen on Figure 5, both cell types demonstrated markedly increased migration in response to the WJ-MSC secretome relative to the untreated control, although the extent of migration was lower than that observed under FBS-supplemented conditions. These findings suggest that the WJ-MSC secretome exerts a stimulatory effect on cell motility in both MSCs and HDFs, consistent with a paracrine-mediated pro-migratory mechanism.

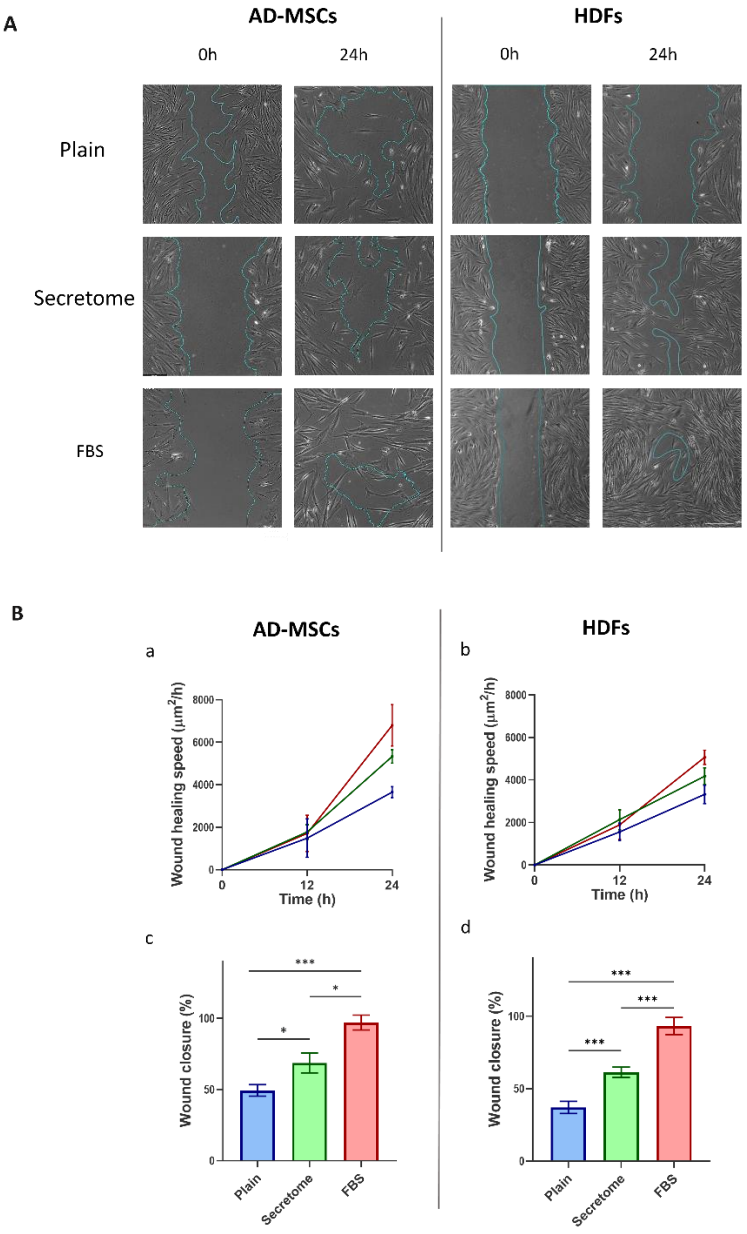

 doi:10.20944/preprints202509.1359.v1

Figure 5. WJ-MSC-derived secretome promotes migration of MSCs and HDFs in an in vitro wound healing assay. Cell migration was evaluated using a scratch assay conducted on collagen-coated substrates over a 24-hour period under three culture conditions: plain medium (Control), medium supplemented with WJ-MSC-derived secretome (Secretome), and medium containing 10% FBS. Panel A shows representative phase-contrast images of AD-MSCs and HDFs at the start of the assay (left) and after 24 hours (right). The initial wound area is marked by a blue line, which also delineates the boundary of the closed region at the endpoint. Panel B quantifies migration dynamics: graphs (a) (AD-MSCs) and (b) (HDFs) display migration speed over time, while graphs (c) (AD-MSCs) and (d) (HDFs) illustrate the percentage of wound closure after 24 hours. Data are color-coded: Control (blue), Secretome-treated (green), and FBS-supplemented (red). Statistical significance is indicated as follows: $p < 0.05$ (*), $p < 0.01$(**) and $p < 0.001$ (***). Scale bar: 20 μm.

4. Discussion

Our findings reveal a robust paracrine interaction between Wharton's WJ-MSCs and adipose-derived AD-MSCs, characterized by enhanced migration, substrate interaction, and extracellular collagen deposition. These effects suggest that MSCs from distinct tissue origins can engage in synergistic signaling, amplifying regenerative outcomes. As specified in the introduction comparative proteomic analyses have shown that WJ-MSC secretome possess a broader and more diverse protein profile than those from adult-derived MSCs, including AD-MSCs, with higher levels of immunomodulatory and pro-regenerative factors such as HGF, VEGF, IL-6, and TGF-β1 [17,42]. This molecular richness may underline the superior bioactivity observed in our experiments.

Insights into MSC–Fibroblast Interactions

While fibroblasts also responded to WJ-MSC secretome, their activation was modest compared to AD-MSCs. This differential responsiveness likely reflects intrinsic differences in cellular plasticity and receptor expression. AD-MSCs, as multipotent progenitors, possess dynamic transcriptional and epigenetic landscapes that allow rapid adaptation to paracrine cues. In contrast, fibroblasts, being more terminally differentiated, exhibit limited transcriptional flexibility and are primarily geared toward ECM maintenance and wound closure. Mechanistic studies have shown that fibroblast activation is tightly regulated by mechanotransduction pathways such as RhoA/ROCK and YAP/TAZ, which respond to substrate stiffness and ECM tension [43]. Moreover, fibroblast-to-myofibroblast transition (FMT), a hallmark of fibrotic remodeling, is often triggered by persistent TGF-β signaling and mechanical stress. Our data suggests that WJ-MSC secretome does not induce this transition, nor excessive collagen secretion, thus preserving fibroblast quiescence while selectively activating progenitor traits in AD-MSCs.

Substrate Effects on Newly Secreted Collagen Organization

Paracrine stimulation influenced both collagen secretion and its spatial organization within the ECM, underscoring the therapeutic relevance of MSC-derived secretomes in ECM-focused regenerative strategies. The use of species-specific collagen substrates, such as RTC, allowed immunological distinction between endogenous human collagen and exogenous scaffold components, providing a refined platform for studying matrix remodeling. However, under our experimental conditions, RTC appeared suboptimal for supporting organized fibrillogenesis of newly secreted collagen. Its lack of native crosslinking and nucleation sites, combined with a pre-adsorbed and non-physiological surface topology, likely disrupted the alignment of secreted collagen, resulting in clustered aggregates rather than structured fibrils. Collagen self-assembly is highly sensitive to substrate architecture, as well as to environmental factors like pH and ionic strength [44]. To enhance ECM remodeling and functional integration, future studies should explore advanced 3D scaffolds such as decellularized human matrices or biomimetic hydrogels, which have demonstrated superior support for collagen alignment and structural organization [45].

 doi:10.20944/preprints202509.1359.v1

Dose Considerations for Clinical Translation

The concentration of secretome applied in vitro does not necessarily reflect its clinical efficacy. Achieving optimal dosing requires a careful balance between biological activity and safety, avoiding both overstimulation and unintended off-target effects. As noted by Gwam et al. (2021) [46], the regenerative potency of MSC-derived secretomes is dose-dependent, with maximal effects typically observed at intermediate concentrations ranging from 50 to 200 μg/mL of total protein. Higher doses may provoke cellular stress or immune activation, while insufficient concentrations may fail to elicit a meaningful therapeutic response. In our study, we utilized the native concentration of secretome present in the conditioned medium collected from WJ-MSCs after 48 hours of culture (approx. 300 μg/ml total protein) prior to any concentration step, thus reflecting a physiologically relevant exposure level. To ensure reproducibility and translational relevance, the standardization of MSC secretome production is essential. This involves tightly controlling variables such as cell density, culture duration, and the composition of the conditioning medium, all of which significantly influence the secretome's bioactivity and therapeutic potential [47,48]. Without harmonized protocols, batch-to-batch variability can compromise both experimental outcomes and clinical efficacy, underscoring the need for GMP-compliant manufacturing strategies [47]. Furthermore, quantitative proteomic profiling and functional bioassays should be employed to define therapeutic windows tailored to specific clinical applications.

Therapeutic Implications of Combinatory MSC Strategies

Our findings support the development of combination MSC therapies that leverage the complementary strengths of different MSC sources. WJ-MSCs offer robust immunomodulatory and proliferative signals, while AD-MSCs contribute lineage-specific differentiation and ECM remodeling. Clinical trials have demonstrated that WJ-MSC-derived exosomes accelerate wound healing and reduce inflammation in diabetic foot ulcers [49], whereas AD-MSCs show promise in cartilage regeneration and osteoarthritis management [50]. A combinatorial approach, either through co-culture, sequential secretome delivery, or engineered hybrid formulations, could enhance therapeutic outcomes by targeting multiple regenerative pathways simultaneously. Furthermore, the ability of WJ-MSC secretome to activate both progenitor and stromal cells suggests a dual mechanism of action: recruiting stem cells to sites of injury while mobilizing resident fibroblasts for matrix reorganization. This aligns with emerging paradigms in regenerative medicine that favor cell-free therapies capable of orchestrating endogenous repair processes without the logistical and immunological challenges of cell transplantation, as highlighted by González-González and colleagues (2020) [51].

Study Limitations

Despite the promising in vitro findings, several limitations must be acknowledged to contextualize the translational relevance of this study.

- In vitro constraints: Our experiments were conducted under controlled in vitro conditions, which do not fully replicate the complexity of in vivo tissue environments. Factors such as immune cell interactions, vascularization, mechanical stress, and systemic feedback loops are absent but play critical roles in regenerative outcomes. In vivo validation using relevant animal models is essential to assess therapeutic efficacy, biodistribution, and long-term safety.
- Donor variability: The composition and potency of MSC secretomes are influenced by donor-specific factors including age, sex, metabolic status, and tissue origin. Proteomic profiling has revealed significant inter-donor variability in the abundance of key regenerative proteins such as VEGF, BDNF, and PDGF-AA [52,53]. This underscores the need for standardized donor selection and quality control protocols in secretome production.
- Time-limited assessment: Our analysis focused on cellular responses within a 72-hour window, capturing early proliferative, migratory, and ECM remodeling events. However, MSC secretome

 doi:10.20944/preprints202509.1359.v1

effects may evolve over longer durations, influencing differentiation, immunomodulation, and tissue integration. Time-course studies extending beyond 72 hours are needed to assess sustained activation, potential senescence, or feedback inhibition mechanisms.

5. Conclusions

This study demonstrates that the WJ-MSC-derived secretome selectively activates AD-MSCs while maintaining fibroblast quiescence, highlighting its potential for anti-fibrotic regenerative therapies. The biphasic cell cycle response in AD-MSCs suggests controlled activation that may preserve stemness and enhance function, contrasting with the static profile of fibroblasts. The use of species-specific collagen substrates enabled a clear distinction between endogenous matrix remodeling and scaffold contributions, offering a methodological advantage for future ECM studies.

Therapeutically, the ability to stimulate AD-MSCs proliferation and migration without triggering fibroblast overgrowth supports the development of combination MSCs strategies that balance immunomodulation and differentiation while minimizing fibrotic risk. These findings reinforce the promise of cell-free regenerative approaches and call for in vivo validation, donor standardization, and long-term assessment to guide clinical translation.

Author Contributions: Conceptualization, G.A.; methodology G.A. and R.K.-P.; methodology, cell culture, writing and software analysis, T.S. and L.T.; collagen investigation, data curation T.S, L.T.; writing original draft preparation, G.A.; writing and editing, G.A., S.T. and R.K.-P.; supervision, G.A.; resources, S.K.; funding acquisition, G.A., P. K-P. and S.T. All authors have read and agreed to the published version of the manuscript.

Funding: This research was funded by the European Union NextGeneration EU, through the National Recovery and Resilience Plan of the Republic of Bulgaria, project BG-RRP-2.004-0003. The financial support of the project BG16RFPR002-1.014-0002-C001 “Centre of competence in personalized medicine, 3d and telemedicine, robotic assisted and minimally invasive surgery” funded by the PRIDST 2021-2027 and co-funded by the EU, is also acknowledged.

Institutional Review Board Statement: This study was conducted according to the guidelines of theDeclaration of Helsinki and approved by the Institutional Ethics Committee of Medical University—Pleven (approval 745-KENID 05/06/23).

Data Availability Statement: The original contributions presented in this study are included in the article. Further inquiries can be directed to the corresponding author.

Acknowledgments: We acknowledge support through Leonardo da Vinci Center of Competence in Personalized Medicine, 3D and Telemedicine, Robotic and Minimally Invasive Surgery, Pleven, Bulgaria.

Conflicts of Interest: The authors declare no conflicts of interest.

Abbreviations

The following abbreviations are used in this manuscript:

WJ-MSCs	Wharton’s Jelly-Derived Mesenchymal Stem Cells
AD-MSCs	Adipose-Derived Mesenchymal Stem Cells
HDFs	Human Dermal Fibroblasts
RTC	Rat Tail Collagen
FBS	Fetal Bovine Serum
MSCs	Mesenchymal Stem Cells
ECM	Extracellular Matrix
PBS	Phosphate Buffered Saline
CSA	Cell Spreading Area
AR	Cell Aspect Ratio
FMT	Fibroblast-to-Myofibroblast Transition

 doi:10.20944/preprints202509.1359.v1

References

1. V. V. Maldonado et al., "Clinical utility of mesenchymal stem/stromal cells in regenerative medicine and cellular therapy," *J Biol Eng*, vol. 17, no. 1, p. 44, Jul. 2023, doi: 10.1186/s13036-023-00361-9.
2. A. C. Pînzariu et al., "The therapeutic use and potential of MSCs: advances in regenerative medicine," *Int J Mol Sci*, vol. 26, no. 7, p. 3084, Mar. 2025, doi: 10.3390/ijms26073084.
3. F. Vizoso, N. Eiro, S. Cid, J. Schneider, and R. Perez-Fernandez, "Mesenchymal stem cell secretome: toward cell-free therapeutic strategies in regenerative medicine," *Int J Mol Sci*, vol. 18, no. 9, p. 1852, Aug. 2017, doi: 10.3390/ijms18091852.
4. A. I. Caplan and D. Correa, "The MSC: An injury drugstore," *Cell Stem Cell*, vol. 9, no. 1, pp. 11–15, Jul. 2011, doi: 10.1016/j.stem.2011.06.008.
5. C. R. Harrell, V. Djonov, and V. Volarevic, "The cross-talk between mesenchymal stem cells and immune cells in tissue repair and regeneration," *Int J Mol Sci*, vol. 22, no. 5, p. 2472, Mar. 2021, doi: 10.3390/ijms22052472.
6. U. Sajjad et al., "Exploring Mesenchymal Stem Cells Homing Mechanisms and Improvement Strategies," *Stem Cells Transl Med*, vol. 13, no. 12, pp. 1161–1177, Dec. 2024, doi: 10.1093/stcltm/szae045.
7. H. Drobiova, S. Sindhu, R. Ahmad, D. Haddad, F. Al-Mulla, and A. Al Madhoun, "Wharton's jelly mesenchymal stem cells: a concise review of their secretome and prospective clinical applications," *Front Cell Dev Biol*, vol. 11, Jun. 2023, doi: 10.3389/fcell.2023.1211217.
8. D. W. Kim, M. Staples, K. Shinozuka, P. Pantcheva, S. D. Kang, and C. V. Borlongan, "Wharton's jelly-derived mesenchymal stem cells: Phenotypic characterization and Optimizing their therapeutic potential for clinical applications," *Int J Mol Sci*, vol. 14, no. 6, pp. 11692–11712, May 2013, doi: 10.3390/ijms140611692.
9. M. Mendiratta et al., "Concurrent hypoxia and apoptosis imparts immune programming potential in mesenchymal stem cells: Lesson from acute graft-versus-host-disease model," *Stem Cell Research and Therapy* , vol. 15, no. 1, Dec. 2024, doi: 10.1186/s13287-024-03947-2.
10. S. B. Shivakumar et al., "DMSO- and Serum-Free Cryopreservation of Wharton's Jelly Tissue Isolated From Human Umbilical Cord," *J Cell Biochem*, pp. 2397–2412, Oct. 2016, doi: 10.1002/jcb.25563.
11. J. Wang and R. Li, "Effects, methods and limits of the cryopreservation on mesenchymal stem cells," Dec. 01, 2024, *BioMed Central Ltd*. doi: 10.1186/s13287-024-03954-3.
12. C. Y. Fong, A. Subramanian, A. Biswas, and A. Bongso, "Freezing of fresh Wharton's Jelly from human umbilical cords yields high post-thaw mesenchymal stem cell numbers for cell-based therapies," *J Cell Biochem*, vol. 117, no. 4, pp. 815–827, Apr. 2016, doi: 10.1002/jcb.25375.
13. M. Ghasemi, E. Roshandel, M. Mohammadian, B. Farhadihosseinabadi, P. Akbarzadehlaleh, and K. Shamsasenjan, "Mesenchymal stromal cell-derived secretome-based therapy for neurodegenerative diseases: overview of clinical trials," Dec. 01, 2023, *BioMed Central Ltd*. doi: 10.1186/s13287-023-03264-0.
14. J. W. Prado-Yupanqui et al., "The Hidden Power of the Secretome: Therapeutic Potential on Wound Healing and Cell-Free Regenerative Medicine—A Systematic Review," *Int J Mol Sci*, vol. 26, no. 5, Feb. 2025, doi: 10.3390/ijms26051926.
15. C. M. Trigo, J. S. Rodrigues, S. P. Camões, S. Solá, and J. P. Miranda, "Mesenchymal stem cell secretome for regenerative medicine: Where do we stand?," *J Adv Res*, vol. 70, pp. 103–124, Apr. 2025, doi: 10.1016/j.jare.2024.05.004.
16. B. Cappe, P. Vandenabeele, and F. B. Riquet, "A guide to the expanding field of extracellular vesicles and their release in regulated cell death programs," May 01, 2024, *John Wiley and Sons Inc*. doi: 10.1111/febs.16981.
17. S. Shin et al., "Comparative proteomic analysis of the mesenchymal stem cells secretome from adipose, bone marrow, placenta and wharton's jelly," *Int J Mol Sci*, vol. 22, no. 2, pp. 1–17, Jan. 2021, doi: 10.3390/ijms22020845.
18. X. Zhang, Y. Zhang, and Y. Liu, "Fibroblast activation and heterogeneity in fibrotic disease," *Nat Rev Nephrol*, Jun. 2025, doi: 10.1038/s41581-025-00969-8.
19. R. Xu et al., "Mesenchymal stem cells reversibly de-differentiate myofibroblasts to fibroblast-like cells by inhibiting the TGF-β-SMAD2/3 pathway," *Molecular Medicine*, vol. 29, no. 1, Apr. 2023, doi: 10.1186/s10020-023-00630-9.

 doi:10.20944/preprints202509.1359.v1

20. U. Dyachkova, M. Vigovskiy, N. Basalova, A. Efimenko, and O. Grigorieva, "M2-macrophage-induced chronic inflammation promotes reversible mesenchymal stromal cell senescence and reduces their anti-fibrotic properties," *Int J Mol Sci*, vol. 24, no. 23, p. 17089, Dec. 2023, doi: 10.3390/ijms242317089.
21. V. D. Desai, H. C. Hsia, and J. E. Schwarzbauer, "Reversible modulation of myofibroblast differentiation in adipose-derived mesenchymal stem cells," *PLoS One*, vol. 9, no. 1, Jan. 2014, doi: 10.1371/journal.pone.0086865.
22. V. B. R. Konala, R. Bhonde, and R. Pal, "Secretome studies of mesenchymal stromal cells (MSCs) isolated from three tissue sources reveal subtle differences in potency," In Vitro *Cell Dev Biol Anim*, vol. 56, no. 9, pp. 689–700, Oct. 2020, doi: 10.1007/s11626-020-00501-1.
23. H. M. Akhir and P. L. Teoh, "Collagen type I promotes osteogenic differentiation of amniotic membrane-derived mesenchymal stromal cells in basal and induction media," *Biosci Rep*, vol. 40, no. 12, Dec. 2020, doi: 10.1042/BSR20201325.
24. K. M. Pawelec, S. M. Best, and R. E. Cameron, "Collagen: a network for regenerative medicine," *J Mater Chem B*, vol. 4, no. 40, pp. 6484–6496, 2016, doi: 10.1039/C6TB00807K.
25. R. Komsa-Penkova, G. Stavreva, K. Belemezova, S. Kyurkchiev, S. Todinova, and G. Altankov, "Mesenchymal stem-cell remodeling of adsorbed type-I collagen—The effect of collagen oxidation," *Int J Mol Sci*, vol. 23, no. 6, Mar. 2022, doi: 10.3390/ijms23063058.
26. C. Somaiah et al., "Collagen promotes higher adhesion, survival and proliferation of mesenchymal stem cells," *PLoS One*, vol. 10, no. 12, p. e0145068, Dec. 2015, doi: 10.1371/journal.pone.0145068.
27. M. Abedi, M. Shafiee, F. Afshari, H. Mohammadi, and Y. Ghasemi, "Collagen-based medical devices for regenerative medicine and tissue engineering," *Appl Biochem Biotechnol*, vol. 196, no. 8, pp. 5563–5603, Dec. 2024, doi: 10.1007/s12010-023-04793-3.
28. K. Gelse, E. Pöschl, and T. Aigner, "Collagens—Structure, function, and biosynthesis," *Adv Drug Deliv Rev*, vol. 55, no. 12, pp. 1531–1546, Nov. 2003, doi: 10.1016/j.addr.2003.08.002.
29. S. Ricard-Blum, "The Collagen Family," *Cold Spring Harb Perspect Biol*, vol. 3, no. 1, pp. 1–19, Jan. 2011, doi: 10.1101/cshperspect.a004978.
30. B. S. Weeks, R. Fu, and M. Zaidi, "Vitamin C promotes wound healing: The use of in vitro scratch assays to assess re-epithelialization," in *Cell Physiology*, vol. 2023, IntechOpen, 2023. [Online]. Available: www.intechopen.com
31. A. Alexandrova-Watanabe et al., "Assessment of Red Blood Cell Aggregation in Preeclampsia by Microfluidic Image Flow Analysis—Impact of Oxidative Stress on Disease Severity," *Int J Mol Sci*, vol. 25, no. 7, Apr. 2024, doi: 10.3390/ijms25073732.
32. C. Frantz, K. M. Stewart, and V. M. Weaver, "The extracellular matrix at a glance," *J Cell Sci*, vol. 123, no. 24, pp. 4195–4200, Dec. 2010, doi: 10.1242/jcs.023820.
33. A. D. Theocharis, D. Manou, and N. K. Karamanos, "The Extracellular Matrix as a Multitasking Player in Disease," *FEBS Journal*, vol. 286, no. 15, pp. 2830–2869, 2019, doi: 10.1111/febs.14818.
34. S. S. Ningsih, S. W. A. Jusman, R. Syaidah, R. Nauli, and F. Fadilah, "Efficient protocol for isolating human fibroblast from primary skin cell cultures: application to keloid, hypertrophic scar, and normal skin biopsies," *Biol Methods Protoc*, vol. 9, no. 1, 2024, doi: 10.1093/biomethods/bpae082.
35. K. Mikulíková, A. Eckhardt, S. Pataridis, and I. Mikšík, "Study of posttranslational non-enzymatic modifications of collagen using capillary electrophoresis/mass spectrometry and high performance liquid chromatography/mass spectrometry," *J Chromatogr A*, vol. 1155, no. 2, pp. 125–133, Jul. 2007, doi: 10.1016/j.chroma.2007.01.020.
36. R. Komsa-Penkova, R. Spirova, and B. Bechev, "Modification of Lowry's method for collagen concentration measurement," *J Biochem Biophys Methods*, vol. 32, no. 1, pp. 33–43, Apr. 1996, doi: 10.1016/0165-022X(95)00046-T.
37. D. R. Stirling, M. J. Swain-Bowden, A. M. Lucas, A. E. Carpenter, B. A. Cimini, and A. Goodman, "CellProfiler 4: improvements in speed, utility and usability," *BMC Bioinformatics*, vol. 22, no. 1, p. 433, Dec. 2021, doi: 10.1186/s12859-021-04344-9.
38. V. Roukos, G. Pegoraro, T. C. Voss, and T. Misteli, "Cell cycle staging of individual cells by fluorescence microscopy," *Nat Protoc*, vol. 10, no. 2, pp. 334–348, Feb. 2015, doi: 10.1038/nprot.2015.016.

 doi:10.20944/preprints202509.1359.v1

39. A. Suarez-Arnedo, F. T. Figueroa, C. Clavijo, P. Arbeláez, J. C. Cruz, and C. Muñoz-Camargo, "An image J plugin for the high throughput image analysis of in vitro scratch wound healing assays," *PLoS One*, vol. 15, no. 7, Jul. 2020, doi: 10.1371/journal.pone.0232565.
40. N. Kalinina et al., "Characterization of secretomes provides evidence for adipose-derived mesenchymal stromal cells subtypes," *Stem Cell Res Ther*, vol. 6, no. 1, Nov. 2015, doi: 10.1186/s13287-015-0209-8.
41. A. Stamm, K. Reimers, S. Strauß, P. Vogt, T. Scheper, and I. Pepelanova, "In vitro wound healing assays—State of the art," *BioNanoMaterials*, vol. 17, no. 1–2, pp. 79–87, May 2016, doi: 10.1515/bnm-2016-0002.
42. D. Kehl et al., "Proteomic analysis of human mesenchymal stromal cell secretomes: a systematic comparison of the angiogenic potential," *NPJ Regen Med*, vol. 4, no. 8, Apr. 2019, doi: 10.1038/s41536-019-0070-y.
43. Y. Chang, J. W. N. Lee, and A. W. Holle, "The mechanobiology of fibroblast activation in disease," *APL Bioeng*, vol. 9, no. 2, p. 021505, Jun. 2025, doi: 10.1063/5.0272393.
44. E. G. Canty and K. E. Kadler, "Procollagen trafficking, processing and fibrillogenesis," *J Cell Sci*, vol. 118, no. 7, pp. 1341–1353, Apr. 2005, doi: 10.1242/jcs.01731.
45. J. González-Masís et al., "Self-assembly study of type I collagen extracted from male Wistar Hannover rat tail tendons," *Biomater Res*, vol. 24, no. 1, Dec. 2020, doi: 10.1186/s40824-020-00197-0.
46. C. Gwam, N. Mohammed, and X. Ma, "Stem cell secretome, regeneration, and clinical translation: a narrative review," *Ann Transl Med*, vol. 9, no. 1, pp. 70–70, Jan. 2021, doi: 10.21037/atm-20-5030.
47. B. Chouaib, M. Haack-Sørensen, F. Chaubron, F. Cuisinier, and P. Y. Collart-Dutilleul, "Towards the standardization of mesenchymal stem cell secretome-derived product manufacturing for tissue regeneration," *Int J Mol Sci*, vol. 24, no. 16, Aug. 2023, doi: 10.3390/ijms241612594.
48. D. Mushahary, A. Spittler, C. Kasper, V. Weber, and V. Charwat, "Isolation, cultivation, and characterization of human mesenchymal stem cells," *Cytometry Part A*, vol. 93, no. 1, pp. 19–31, Jan. 2018, doi: 10.1002/cyto.a.23242.
49. A. Hafez, "Efficacy and safety of Wharton's jelly-derived mesenchymal stem cell exosomes in the treatment of diabetic foot ulcers: a double-blinded randomized controlled clinical trial (WJ-MSC)," Apr. 2025.
50. H. Sun et al., "Clinical outcomes of autologous adipose-derived mesenchymal stem cell combined with high tibial osteotomy for knee osteoarthritis are correlated with stem cell stemness and senescence," *J Transl Med*, vol. 22, no. 1039, Nov. 2024, doi: 10.1186/s12967-024-05814-3.
51. A. González-González, D. García-Sánchez, M. Dotta, J. C. Rodríguez-Rey, and F. M. Pérez-Campo, "Mesenchymal stem cells secretome: The cornerstone of cell-free regenerative medicine," *World J Stem Cells*, vol. 12, no. 12, pp. 1439–1690, 2020, doi: 10.4252/wjsc.v12.i12.1529.
52. M. Koczkowska et al., "Identifying differentiation markers between dermal fibroblasts and adipose-derived mesenchymal stromal cells (AD-MSCs) in human visceral and subcutaneous tissues using single-cell transcriptomics," *Stem Cell Research and Therapy* , vol. 16, no. 1, Feb. 2025, doi: 10.1186/s13287-025-04185-w.
53. S. Nováková et al., "Proteomic study revealed a distinction between human dermal Fibroblasts and Mesenchymal Stem Cells from Different Sources," *Stem Cell Rev Rep*, Jun. 2025, doi: 10.1007/s12015-025-10926-4.